

Electronic Supplementary Material

Calibrating SECCM measurements by means of a nanoelectrode ruler. The intrinsic oxygen reduction activity of PtNi catalyst nanoparticles

Emmanuel Batsa Tetteh^{1,§}, Tobias Löffler^{1,§}, Tsvetan Tarnev¹, Thomas Quast¹, Patrick Wilde¹, Harshitha Barike Aiyappa¹, Simon Schumacher², Corina Andronesu², Richard D. Tilley³, Xingxing Chen⁴ (✉), Wolfgang Schuhmann¹ (✉)

¹ Analytical Chemistry–Center for Electrochemical Sciences, Faculty of Chemistry and Biochemistry, Ruhr University Bochum, Universitätsstr. 150, D-44780 Bochum, Germany

² Chemical Technology III, Faculty of Chemistry and CENIDE–Center for Nanointegration, University Duisburg Essen, Carl Benz Str. 199, D-47057 Duisburg, Germany

³ School of Chemistry and Australian Centre for NanoMedicine, University of New South Wales, Sydney 2052, Australia

⁴ Research Group of Functional Materials for Electrochemical Energy Conversion, School of Chemical Engineering, University of Science and Technology Liaoning, 114051 Anshan, China

[§] Emmanuel Batsa Tetteh and Tobias Löffler contributed equally to this work.

Supporting information to <https://doi.org/10.1007/s12274-021-3702-7>

Nanoparticle Characterisation

The synthesised PtNi₂ NPs have been evaluated regarding their size distribution and composition (EDS) via (S)TEM analysis on a flat TEM grid as described in the Experimental Section (**Figure S1**). A diameter of about 9 nm was revealed with no investigated NP being smaller than 5 nm or bigger than 13 nm in diameter. EDS confirms the elemental composition of the NPs as PtNi₂ NPs.

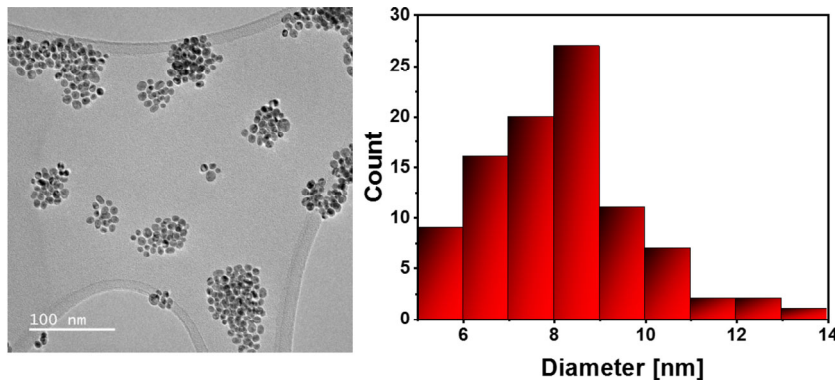


Figure S1 TEM image of PtNi₂ nanoparticles on a TEM grid and the corresponding particle size distribution determined with the software ImageJ.

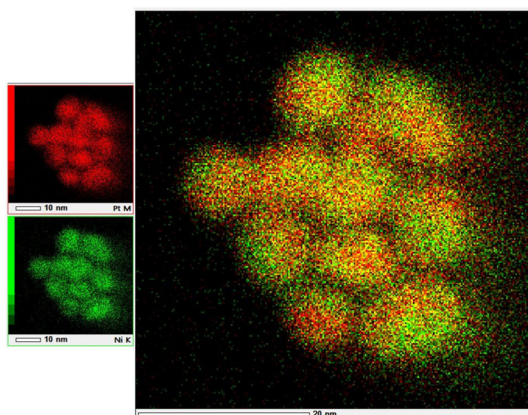


Figure S2 STEM-EDS image of PtNi₂ nanoparticles on a TEM grid confirming the aspired NP composition.

Address correspondence to Xingxing Chen, xingchenstar79@163.com; Wolfgang Schuhmann, wolfgang.schuhmann@rub.de

Imaging of the SECCM tip opening

The wetted area during the electrochemical measurement is approximately in the range of the micropipette opening. Hence, we considered its diameter as an approximate diameter of the active wetted electrode area of each spot, which allowed to clearly conclude a significantly less-than-a-monolayer coverage of PtNi₂ NPs at each spot.

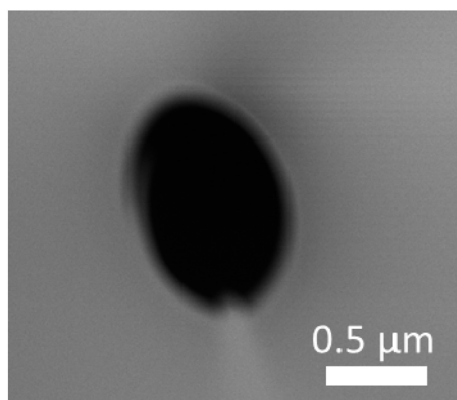


Figure S3 SEM micrograph of the glass micropipette opening used in the SECCM measurement with a diameter of about 800 nm.

Recording possible reference electrode potential shift via a stable redox mediator

To rule out any reference electrode potential shift possibly deteriorating the data, we added a free-diffusing Os-complex with well-defined redox behaviour [1] to the electrolyte in the SECCM pipette and performed a CV after the ORR LSV at each spot. The potential between oxidative and reductive peak does not shift upon screening, indicating a stable redox potential within the timeframe of the experiment.

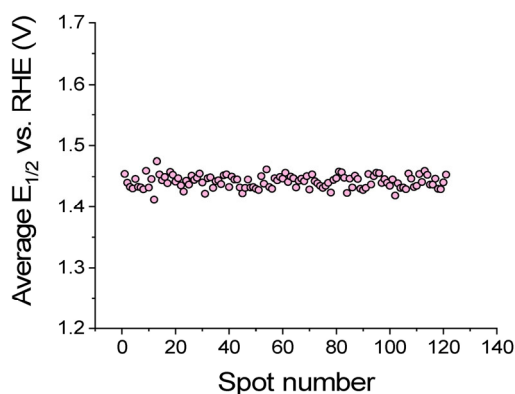


Figure S4 Tracking of the potential between oxidative and reductive wave of an Os(II)-mediator in a ORR-neutral region at each spot. The constant value confirms a stable reference electrode potential.

LSC curves of 121 SECCM spots

The SECCM ORR LSVs at each spot are shown before (a) and after subtraction of the averaged blank electrode response (thick black line). Differences in current are due to differences in NP loading at each spot. Tafel analysis of the electrode corrected LSVs shows a linear correlation for the entire investigated potential range, confirming the analysis of the kinetic properties as well as a successful electrode contribution subtraction, since no combined response of two different materials can be observed.

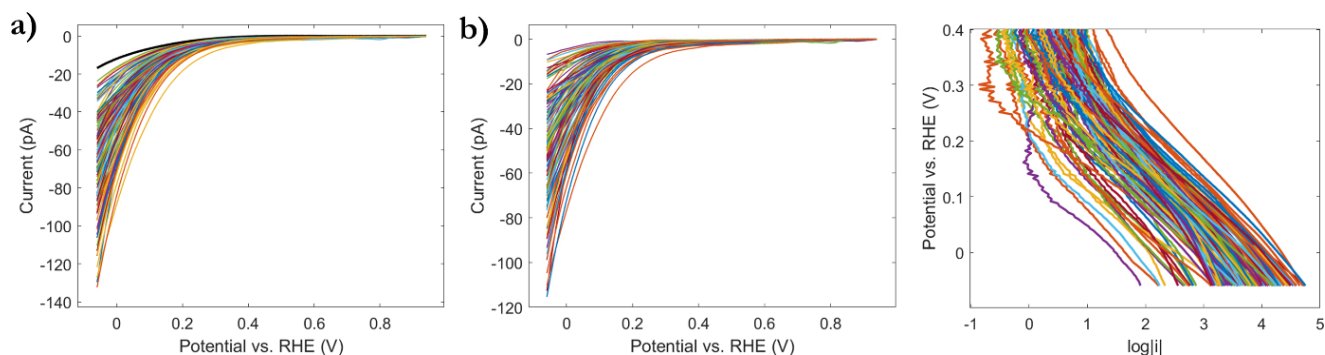


Figure S5 PtNi₂/BDD LSV curves (a) before and (b) after bare electrode correction. The thick black curve in (a) is the average LSV of the bare BDD electrode. Tafel analysis of the electrode corrected curves show Butler-Volmer behaviour confirming the kinetic regime.

Experimental Part:

PtNi₂ nanoparticle synthesis. PtNi₂ nanoparticles were prepared following a synthesis procedure adapted from literature. [2,3] Briefly, 0.19 g of Ni(acac)₂ and 0.15 g Pt(acac)₂ were dissolved in 15 mL oleylamine. Under stirring and vacuum the temperature was raised to 100 °C and kept for 30 min at these conditions. Under argon flow the temperature was raised to 300 °C and kept for 60 min. The mixture was then cooled down to room temperature. The resulting NPs were washed with ethanol to remove excess of surfactant and kept in hexane.

SECCM measurement. A quartz micropipette (for fabrication see below) with tapered opening of ~1 μm was silanised to enhance the hydrophobicity of the tip. This helps to maintain a stable meniscus during SECCM scanning. The silanising was done by dipping the micropipette tip in dichlorodimethylsilane (99%, Acros Organics), for 30 s while applying 6.5 bar of Ar pressure to the rear-end followed by vertical drying in air for 1 min. The micropipette was filled with the electrolyte solution using a MicroFil syringe with a 0.1 mm inner diameter (MF34G-5, World Precision Instruments). A Pt wire with diameter of ca. 0.25 mm was inserted. Before the measurement, the open-circuit potential of the Pt wire vs. a standard Ag/AgCl [3M KCl] reference electrode was determined to calibrate the Pt QRCE.

In brief, a Ag/AgCl [3M KCl] electrode and the electrolyte filled SECCM probe with the Pt wire inserted were placed inside a one-compartment electrochemical cell filled with the same electrolyte solution as in the SECCM probe. Open-circuit potential between the two electrodes was measured by means of a digital potentiometer, which gives the potential value correction factor for calibrating the Pt wire electrode. The working electrode potentials were converted to the RHE reference scale using the equation below.

$$E_{RHE} = E + E_{Ag/AgCl[3MKCl]} + E_{opencircuitpotentialcorrectionfactor} + 0.059(pH)$$

Where E is the potential applied to the working electrode, $E_{Ag/AgCl[3MKCl]} = 0.210$ V, pH of the electrolyte is 13 and the open circuit potential correction factor was consistently found to be 0.043 ± 0.002 . The electrolyte used in this study is a solution containing 0.1 mM [(Os (2,2'-bipyridine)₂(N,N'-dimethyl-2,2'-biimidazole)] (PF₆)₃ in 0.1 M KOH. The Osmium complex served as an internal standard to track the potential drift of the QRCE as shown in our previous study. [1]

The prepared tip was mounted into the SECCM positioning system consisting of step motors (Owis) combined with a high-resolution piezo-electric X-Y-Z-positioning system (P-611.3S nanocube with E-664 amplifier, Physik Instrumente). An optical video microscope (DMK 21AU04, The Imaging Source) using the software IP Capture 2.4 was utilized to monitor the proximity of tip and substrate during the initial positioning. The set-up is installed in a Faraday cage equipped with thermal isolation panels (Vaku-Isotherm) placed on a vibration damping table (RS 2000, Newport) with four S-2000 stabilizers (Newport) to decouple it from vibrations of the building. The WE potential was controlled, with respect to the Pt QRCE and the current flowing at the QRCE (i.e., i_{surf}), was measured using a variable gain transimpedance amplifier (DLPCA-200, FEMTO Messtechnik).

For SECCM measurements, the SECCM probe was positioned ca. 50 μm above the working electrode which was either a bare boron-doped diamond electrode (BioLogic, <https://www.biologic.net/accessory/working-electrodes/>) or PtNi₂ nanoparticles deposited on the same boron-doped diamond electrode.

The measurements were performed in hopping-mode. The SECCM probe was approached to the WE surface using a surface current (i_{surf}) threshold of ca. 2 pA to detect when the meniscus-surface contact had been made and to stop further translation. Note that the SECCM probe itself never contacted the WE surface. A linear sweep voltammogram (LSV) in the potential range of 0 to -1 V vs. Pt was recorded for the oxygen reduction reaction followed by 3 cyclic voltammograms with scan rates of 0.5, 1 and 2 V/s within the potential window of the internal standard (0 – 0.8 V vs. Pt). After the electrochemical measurement, the probe is lifted by a pre-set distance of 2 μm and moved to the next site 4 μm away, where the procedure is repeated to acquire another electrochemical measurement. The tip positioning, electrochemical measurement and data acquisition are automatically controlled by an FPGA card (PCIe-7852R; National Instruments) through a modified version of the open source WEC-SPM software provided by Prof. Patrick Unwin, Warwick University. An area of 40×40 μm² was scanned with 4 μm increments in each direction yielding 121 (11 by 11) independent measurements per scan. The duration of each scan was ca. 30 min. The Pt QRCEs were found to be stable within the timeframe of the SECCM scans (Figure S4).

SECCM capillary fabrication. Single-barrelled SECCM probes were fabricated from quartz filamented capillaries (ZQF-120-90-10, Science Products) using a CO₂-laser puller (P-2000, Sutter Instruments). The pipettes were highly reproducible with tip diameters of approximately 1 μm characterized using SEM. Pulling parameters are: Heat 720, Filament 4, Velocity 40, Delay 130, Pull 100.

Carbon nanoelectrode fabrication and FIB-processing. Quartz glass capillaries (outer diameter 1.2 mm, inner diameter 0.9 mm, length 7.5 cm from Science Products) were pulled using a laser puller P2000 (Sutter Instruments) to fabricate capillaries with nanometre sized tip diameters. [4] The carbon nano electrodes (CNEs) are fabricated by depositing carbon inside these capillaries in a controlled two-step pyrolysis protocol employing a fully automatized set-up as described in. [5] A mixture of propane (Air Liquide, technical grade) and n-butane (Air Liquide, 99.5%) under a protective argon counter-flow atmosphere (Air Liquide, 99.999%, 50 mL/min) is used in the pyrolysis process to form a conductive carbon inside the capillary.

The as-produced electrodes were further processed using focused ion beam (FIB) milling inside the scanning electron microscope (SEM). The electrodes were positioned with their orifice in an 45° angle relative to the Ga⁺-ion source of the FIB. The FIB milling process was performed using a Ga⁺-ion beam (30 kV acceleration voltage, 100 pA current) for several seconds on the CNE, resulting in nanometre-sized carbon electrode offering a carbon disk with a slant of 45°.

Potential-assisted immobilization

For preparation of the NP suspension, spatula tip of the PtNi₂ NP powder was transferred to a falcon tube and 2 ml EtOH (AnalaR Normapur/vwr chemicals - absolute), 1 ml 0.1 M KOH (Algin, 99.5 %) and 1 droplet of oleylamine (Sigma Aldrich) were added.

After thorough shaking, the suspension was tip sonicated for 10 min at 40 % amplitude using a Sonopuls HD 3100 (Bandelin). 1 ml of the NP suspension taken from the upper volume part was transferred into a vial. Potential-assisted immobilization was performed by positioning of the fibbed carbon nanoelectrode into the NP suspension using a stepper motor. Immobilization is based on statistical collisions of NPs with the electrode due to Brownian motion and sticking by electrostatic interaction at the applied potential with respect to the zeta potential of the NPs. For more detailed information, we refer to [6]. A miniaturised Ag/AgCl (3 M KCl) reference electrode and a carbon cloth located in a second compartment were used as reference and counter electrode, respectively. Immobilization was performed for 5 min at -400 mV vs. Ag/AgCl (3 M KCl).

Electrocatalytic measurement employing the fibbed carbon nanoelectrode

The electrocatalytic measurements were performed in the same cell using the same electrodes as for the immobilization. However, 0.1 M KOH (Algin, 99.5 %) was used as electrolyte. Prior to the NP immobilization, the blank electrode was scanned for 10 cycles to ensure a stable current response. The last cycle served as “electrode current”. This linear sweep voltammogram (LSV) was subtracted from the LSV after NP immobilization to yield the “electrode corrected” activity curve solely representing the NP response. [7,8] For removal of the oleylamine, the electrode with immobilised NPs was removed from the electrolyte and annealed for 2 h at 200 °C under ambient air conditions.

TEM analysis of immobilized nanoparticles

The NP decorated CNE was investigated inside the transmission electron microscope (TEM) employing the scanning transmission electron microscope (STEM) mode coupled with energy dispersive X-Ray spectroscopy (EDS) analysis to obtain the precise number of NP participating in the reaction. The electrode was positioned in the TEM using a custom-built electrode holder [6] in a way that the slanted carbon disc was penetrated by the electrons from the “top” which means the slant of the electrode is following the Z-Height in the TEM. Therefore, one can follow the carbon surface of the electrode and the particles attached on it along the whole slant by changing the Z-Height (adjusting the focus of the TEM). The very end of the exposed carbon disc was focused and then the slant was followed by constantly adjusting the focus of the TEM. Doing so one can distinguish between the particles attached on the carbon disc (in focus and participating in the reaction) and the particles attached on the glass wall of the capillary on the backside of the electrode (out of focus and not participating in the reaction). Combining the result of this approach with the EDS map of the CNE makes the counting of the particles feasible.

Instruments

Scanning electron micrographs were recorded and FIB milling was performed using a Quanta 3D eSEM which is equipped with a Ga⁺-FIB source (FEI) at 30 kV in the high vacuum mode. Electrostatic charging of the carbon nanoelectrodes was prevented by inserting a copper wire from the back end of the capillary. Transmission electron microscopy (TEM) was performed using a JEOL microscope (JEM-2800) equipped with a Schottky-type emission source working at 200 kV. Energy dispersive spectroscopy (EDS) elemental mapping was performed using double silicon drift detectors (SDD), with a solid angle of 0.98 steradians with a detection area of 100 mm².

References

- [1] Tarnev, T.; Aiyappa, H. B.; Botz, A.; Erichsen, T.; Ernst, A.; Andronescu, C.; Schuhmann, W. SECCM investigation of single ZIF-derived nanocomposite particles as oxygen evolution electrocatalysts in alkaline media. *Angew. Chem.* **2019**, *58*, 14265–14269.
- [2] Yu, Y.; Yang, W.; Sun, X.; Zhu, W.; Li, X.-Z.; Sellmyer, D. J.; Sun, S. Monodisperse MPt (M = Fe, Co, Ni, Cu, Zn) nanoparticles prepared from a facile oleylamine reduction of metal salts. *Nano letters* **2014**, *14*, 2778–2782.
- [3] Benedetti, T. M.; Andronescu, C.; Cheong, S.; Wilde, P.; Wordsworth, J.; Kientz, M.; Tilley, R. D.; Schuhmann, W.; Gooding, J. J. Electrocatalytic nanoparticles that mimic the three-dimensional geometric architecture of enzymes: Nanozymes. *J. Am. Chem. Soc.* **2018**, *140*, 13449–13455.
- [4] Actis, P.; Tokar, S.; Clausmeyer, J.; Babakinejad, B.; Mikhaleva, S.; Cornut, R.; Takahashi, Y.; López Córdoba, A.; Novak, P.; Shevchuck, A. I. et al. Electrochemical nanopores for single-cell analysis. *ACS Nano* **2014**, *8*, 875–884.
- [5] Wilde, P.; Quast, T.; Aiyappa, H. B.; Chen, Y.-T.; Botz, A.; Tarnev, T.; Marquitan, M.; Feldhege, S.; Lindner, A.; Andronescu, C. et al. Towards reproducible fabrication of nanometre-sized carbon electrodes: Optimisation of automated nanoelectrode fabrication by means of transmission electron microscopy. *ChemElectroChem* **2018**, *5*, 3083–3088.
- [6] Wilde, P.; Barwe, S.; Andronescu, C.; Schuhmann, W.; Ventosa, E. High resolution, binder-free investigation of the intrinsic activity of immobilized NiFe LDH nanoparticles on etched carbon nanoelectrodes. *Nano Res.* **2018**, *11*, 6034–6044.
- [7] Löffler, T.; Wilde, P.; Öhl, D.; Chen, Y.-T.; Tschulik, K.; Schuhmann, W. Evaluation of the intrinsic catalytic activity of nanoparticles without prior knowledge of the mass loading. *Faraday Discuss.* **2018**, *210*, 317–332.
- [8] Löffler, T.; Meyer, H.; Savan, A.; Wilde, P.; Garzón Manjón, A.; Chen, Y.-T.; Ventosa, E.; Scheu, C.; Ludwig, A.; Schuhmann, W. Discovery of a multinary noble metal-free oxygen reduction catalyst. *Adv. Energy Mater.* **2018**, *8*, 1802269.